Electronic Supplementaly Information

Pushing up the efficiency of planar perovskite solar cells to 18.2% with organic small molecular as electron transport layer

Pei-Yang Gu,[a‡] Ning Wang,[b‡] Chengyuan Wang,[f] Yecheng Zhou,[a] Guankui Long,[a] Miaomiao Tian,[a] Wangqiao Chen,[a] Xiao Wei Sun,[c] Mercouri G. Kanatzidis*[,e] Qichun Zhang,*[,a,d]*

[a]School of Materials Science and Engineering, Nanyang Technological University, Singapore 639798

[b]School of Electrical and Electronic Engineering, Nanyang Technological University, Singapore 639798

[c]Department of Electrical and Electronic Engineering, College of Engineering, South University of Science and Technology of China, Shenzhen 518055, P.R. China

[d]Division of Chemistry and Biological Chemistry, School of Physical and Mathematical Sciences, Nanyang Technological University, Singapore 637371

[e]Department of Chemistry, Northwestern University, 2145 North Sheridan Road, Evanston, IL 60208, USA.

[f]School of Chemistry, The University of Melbourne, Parkville, Victoria, 3010, Australia

Dr P.-Y Gu and Dr N. Wang contributed equally to this work.

Contents

Experimental Section

Materials: poly(3,4-ethylenedioxythiophene) polystyrene sulfonate (PEDOT:PSS, Clevios P VP Al 4083) was purchased from H. C. Starck, Clevios GmbH. Phenyl-C61-butyric acid methyl ester was purchased from NanoC and used as received. Thiophene and 4,7-dibromobe-nzo[*c*][1,2,5]thiadiazole were purchased from Alfa Aesar.1,10-Phenanthroline, 2-ethylhexyl bromide, trimethyltin chloride and *n*-butyllithium were purchased from Sigma-Aldrich Company. 4,7-bis(5-(2-ethylhexyl)thiophen-2-yl)benzo[*c*][1,2,5]thiadiazole-5,6-diamine was synthesized according to the reported procedure.[1]Dichloromethane was distilled from calcium hydride. Tetrahydrofuran was distilled from sodium. Other chemicals and solvents were used directly without further purification.

Characterization: Using $CDCl_3$ as solvents and tetramethylsilane (TMS) as the internal standard, ^1H NMR and ^{13}C NMR spectra were measured on a Bruker Advance 300 NMR spectrometer at ambient temperature. UV-Vis absorbance was recorded on UV-Vis-NIR spectrometer Cary 5000. High resolution mass spectrum (HRMS) was performed on a Waters Q-Tof premier mass spectrometer. Cyclic voltammetry measurements were conducted on a CHI 604E electrochemical analyser with glassy carbon (diameter: 1.6 mm; area: 0.02 cm^2) as a working electrode, and platinum wires as a counter electrode and a reference electrode, respectively. Fc^+/Fc was used as an internal standard. Potentials were recorded versus Fc^+/Fc in a solution of anhydrous dichloromethane (DCM) with 0.1 M tetrabutylammoniumhexafluorophosphate ($TBAPF_6$) as a supporting electrolyte at a scan rate of 100 mV s^{-1}. Employing empirical formulas $E_{LUMO/HOMO}$= -[4.8-E_{Fc} + $E_{re/ox}^{onset}$] eV, where E_{Fc}= 0.24 V (measured in our setup), the value of HOMO or LUMO can be calculated.

The surface morphology of **TDTP** thin film was analysed using atomic force microscope (Park System Co.). The current density-voltage (*J-V*) of the solar cells were measured using a Keithley 2400 source meter under simulated AM1.5 illumination (100 mW cm^{-2}) by a Xenon-lamp-based solar simulator (Solar Light Co.

Inc., USA). The light intensity was calibrated using a Si-reference cell certified by the National Renewable Energy Laboratory, with the mismatch factor less than 2%. A non-reflective mask (0.09 cm^2) was used for defining the cell area. The external quantum efficiency spectra were recorded with an EQE measurement system (PVE 300, Bentham, UK) comprised of a Xenon lamp, a momochoromator, a chopper, a lock-in amplifier, and a calibrated silicon photodetector.

Device fabrication: The pre-patterned ITO (sheet resistance of 15 Ω sq^{-1}, Lumtec, Taiwan) patterned glass were cleaned ultrasonically with an alconox (detergent) solution, followed by sonication in sequence with deionized water, acetone, and isopropyl alcohol for 15 min each, then the substrates were dried using blowing nitrogen gas. The ITO glasses are then UV-ozone treated for 20 mins prior to the deposition of other layers. A ~30 nm-thick poly(3,4-ethylenedioxythiophene) polystyrene sulfonate (PEDOT:PSS) hole transport layer was spun on the top of indium tin oxide (ITO) glass substrate at 3000 rpm for 60 s in ambient conditions, following an annealing treatment at 130 °C for 30 min in air. A 350 nm-thick perovskite ($CH_3NH_3PbI_3$) layer was spun on PEDOT:PSS hole transport layer in glove box using 40 wt.% precursor with equal molar CH_3NH_3I and PbI_2 in DMF solution. The as-spun perovskite layer was annealed at 100 °C for 5 min to drive off solvent and form the perovskite phase. Different thickness of **TDTP** was spun on top of perovskite layer using a solution of **TDTP** in 1,2-dichlorobenzene. The thickness of **TDTP** was carefully carried out using Alpha-Step D-600 Stylus Profiler (KLA-Tencor Corporation). The device (active area: 3.2 mm × 3.2 mm) was completed by the thermal evaporation of the LiF (1 nm)/Al(100 nm) electrode on the top.

Simulation details: The size of the unit cell is determined to avoid the interaction between molecules and perovskite layers. The area of 25.284× 25.029$Å^2$ is the area of a 4×4 110-perovksite surface. The 35.411Å height is set to avoid the interaction between molecules and the other surface. Usually, the interaction cut-off distance should be larger than 10Å. As shown in Figure 5, the distances between the molecules and the other surface are 11.8 Å and 14.0 Å. The cut-off energy was 400 eV. The used **K**-points just the Γ point due to the huge unit cell. The *ab initio* molecular dynamic

simulations temperature is 1000 K, the time interval is 1.0 fs, and the total simulation time is longer than 500 fs, which depends on the energy variation. The **PYPH** and **TDTP** absorption models include 538 and 527 ions, respectively.

Figure S13 shows the energy and temperature a **PYPH** molecule on a 4 ×4 110-perovksite surface during the NVT MD simulations. The absorption system is unstable before 150 fs and reached relative stable equilibrium after 400 fs. A low energy configuration was chosen from MD process as the absorption configuration. Then the chosen configuration was optimized. It converged very slowly due to the very large model.

Synthesis of 10,14-bis(5-(2-ethylhexyl)thiophen-2-yl)dipyrido[3,2-*a*:2',3'-*c*][1,2,5]thiadiazolo[3,4-*i*]phenazine (TDTP)

A mixture of 4,7-bis(5-(2-ethylhexyl)thiophen-2-yl)benzo[*c*][1,2,5]thiadiazole-5,6-diamine (554 mg, 1 mmol) and 1,10-phenanthroline-5,6-dione (210 mg, 1 mmol) in acetic acid (100 mL) was stirred at 118°C under nitrogen for 48 h. After cooling to room temperature, the mixture was poured into methanol and the crude product was purified by column chromatography over silica gel, eluting with DCM/methanol to give green compound **TDTP** (378 mg, 0.52mmol, 52%).

^{1}H NMR (300 MHz, $CDCl_3$) δ 9.05 (t, *J* = 5.4 Hz, 4H), 8.41 (s, 2H), 7.40 (s, 2H), 6.57 (s, 2H), 2.67 (s, 4H), 1.58 – 1.18 (m, 18H), 1.05 – 0.88 (m, 12H).

^{13}C NMR (75 MHz, $CDCl_3$) δ 152.1, 150.5, 150.2, 148.8, 140.7, 135.2, 134.1, 133.8, 133.2, 127.4, 125.3, 123.6, 119.6, 41.4, 33.6, 32.7, 29.1, 25.6, 23.0, 14.3, 11.0.

HR-MS, calcd for $C_{42}H_{45}N_6S_3$, 729.2868; found, 729.2844.

Synthesis of 10,17-bis((triisopropylsilyl)ethynyl)dipyrido[3,2-*a*:2',3'-*c*]quinoxalino[2,3-*i*]phenazine (PYPH)

PYPH was obtained as black powder in 57% yield from the reaction between 1,4-bis((triisopropylsilyl)ethynyl)phenazine-2,3-diamine and 1,10-phenanthroline-5,6-dione by following the general procedure described for **TDTP**.

^{1}H NMR (300 MHz, $CDCl_3$) δ 9.81 (d, *J* = 8.0 Hz, 1H), 9.31 (s, 1H), 8.29 (dt, *J* = 5.8, 2.9 Hz, 1H), 7.92 (dd, *J* = 6.9, 3.4 Hz, 1H), 7.81 (s, 1H), 1.43 (s, 21H).

^{13}C NMR (300 MHz, $CDCl_3$) δ 153.4, 149.4, 145.3, 143.5, 143.1, 141.9, 134.9, 132.2, 130.5, 127.8, 124.5, 123.0, 111.7, 102.4, 19.0, 11.8.

HR-MS, calcd for $C_{46}H_{53}N_6Si_2$, 745.3870; found, 745.3864.

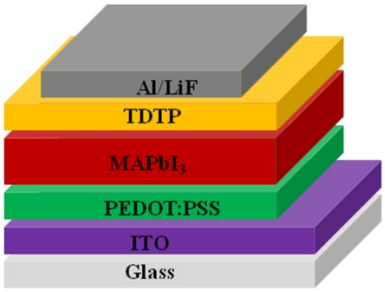

Scheme S1. Device architecture used in this work.

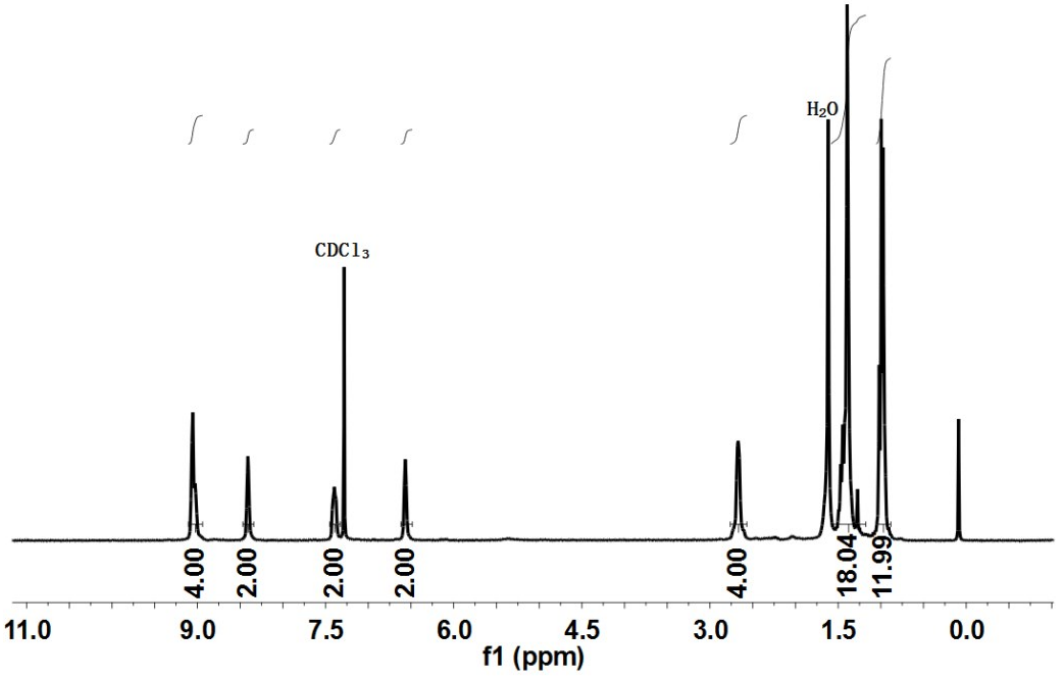

Figure S1.^{1}H NMR spectrum of **TDTP** in $CDCl_3$.

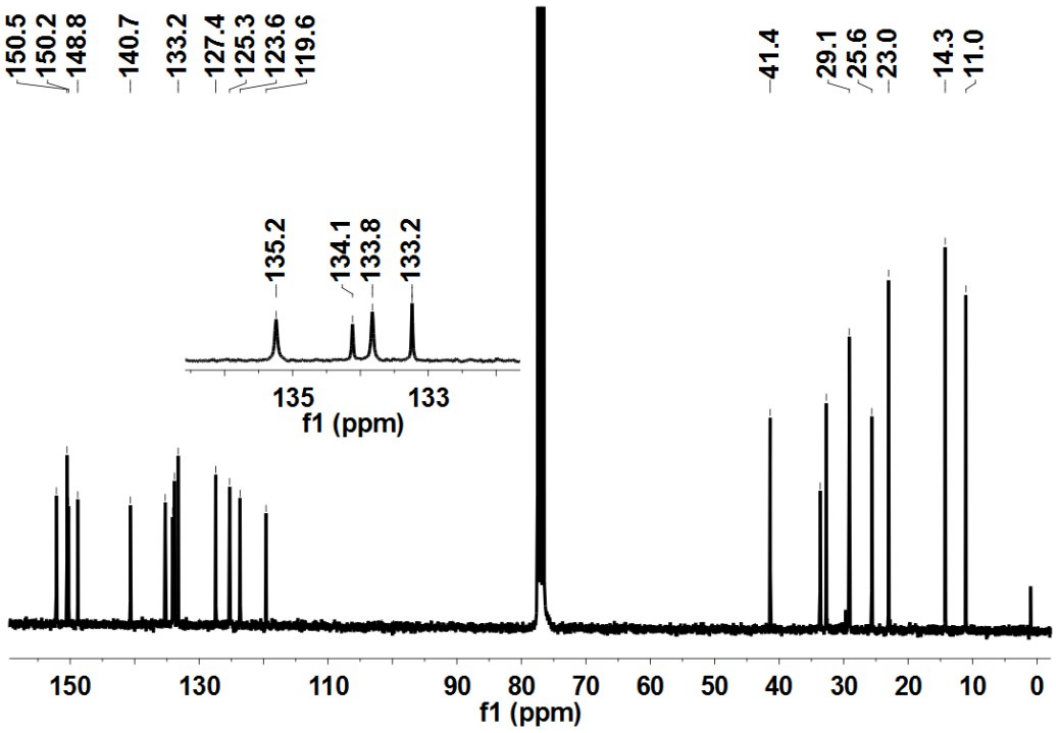

Figure S2. ^{13}C NMR spectrum of **TDTP** in $CDCl_3$.

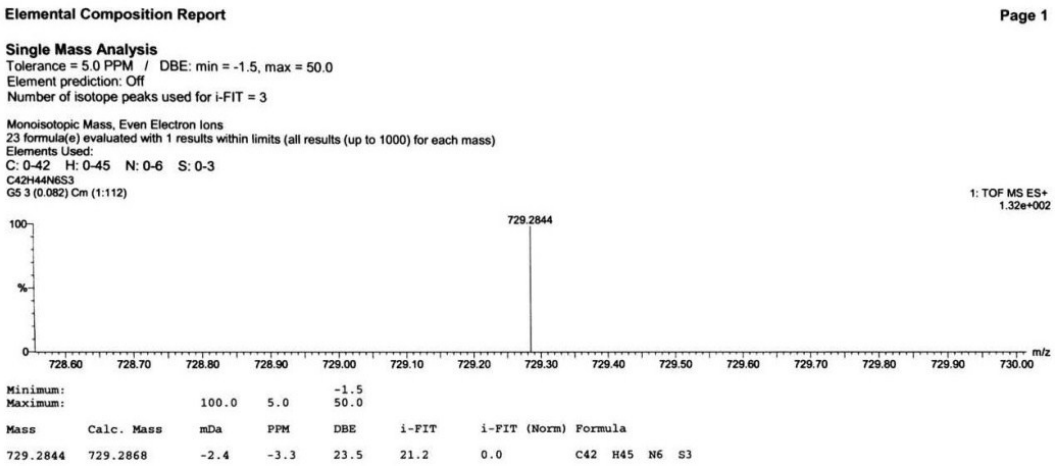

Figure S3. HR-MS of **TDTP**.

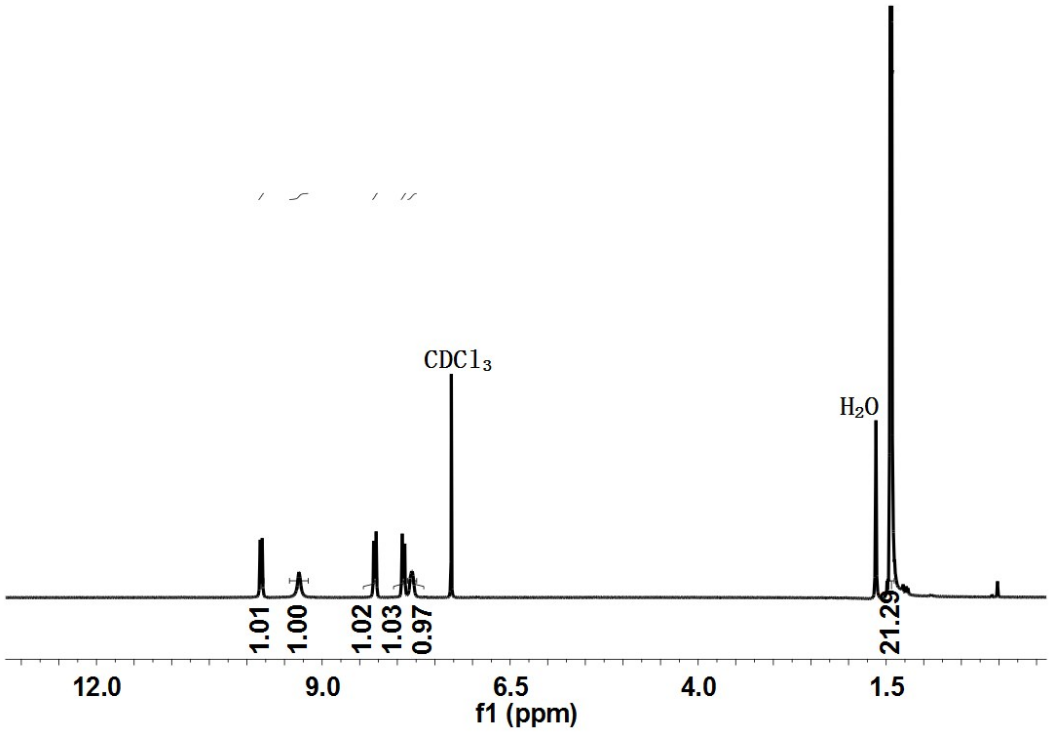

Figure S4.[1]H NMR spectrum of **PYPH** in $CDCl_3$.

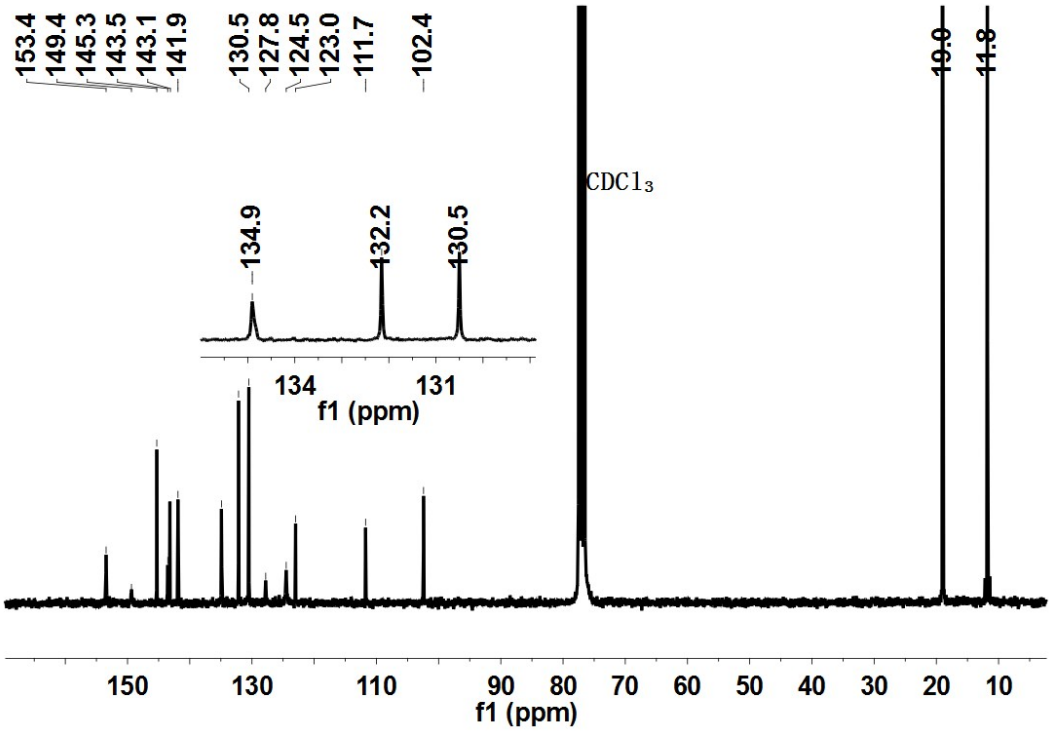

Figure S5.[13]C NMR spectrum of **PYPH** in $CDCl_3$.

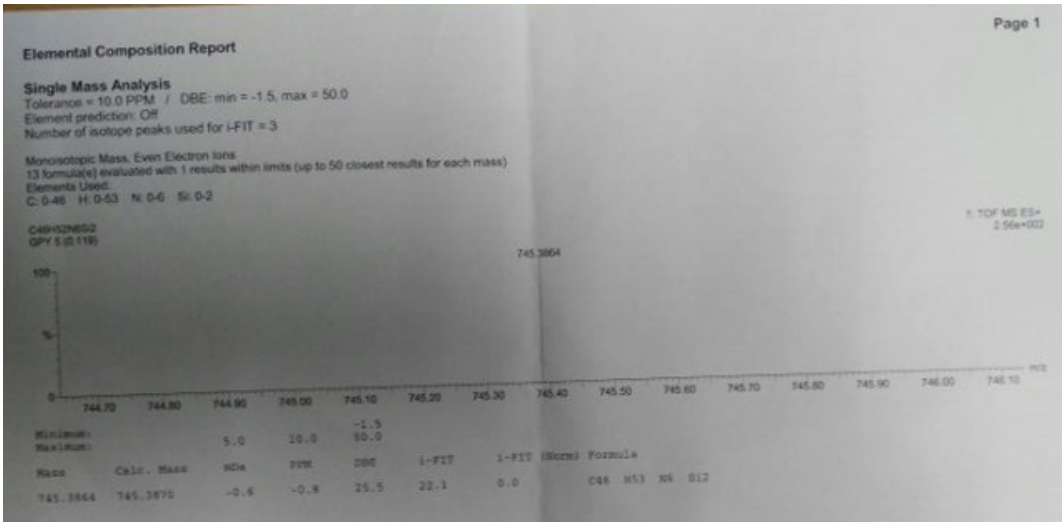

Figure S6. HR-MS of **PYPH**.

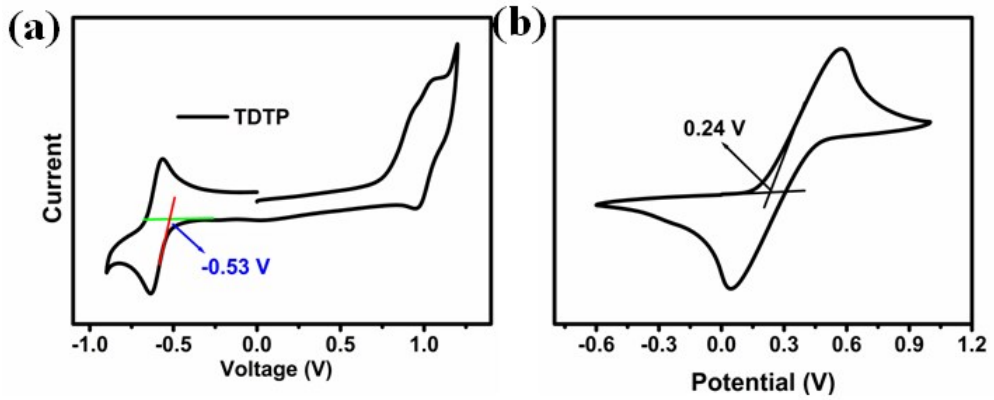

Figure S7.Cyclic voltammograms of (a) **TDTP** and (b) ferrocene in DCM solution.

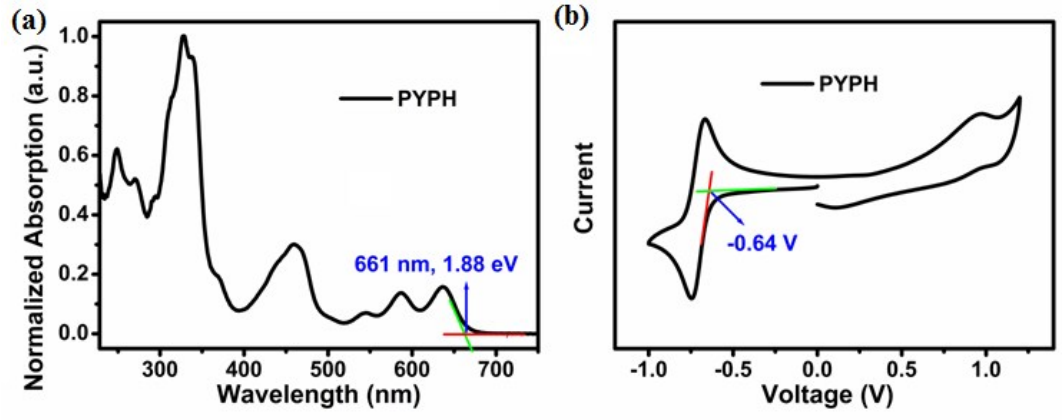

Figure S8. (a) Normalized absorption of **PYPH** in DCM solution; (b) Cyclic voltammograms of **PYPH** in DCM solution.

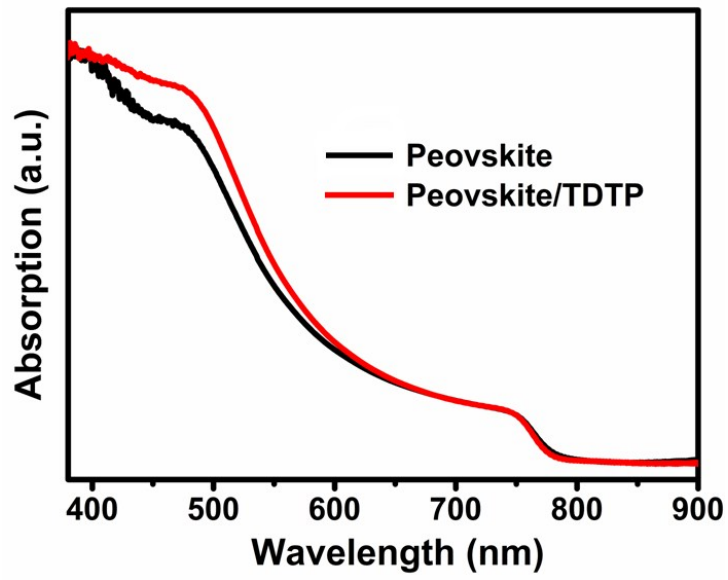

Figure S9. Absorption curves of pure perovskite and bilayer perovskite/**TDTP** thin films.

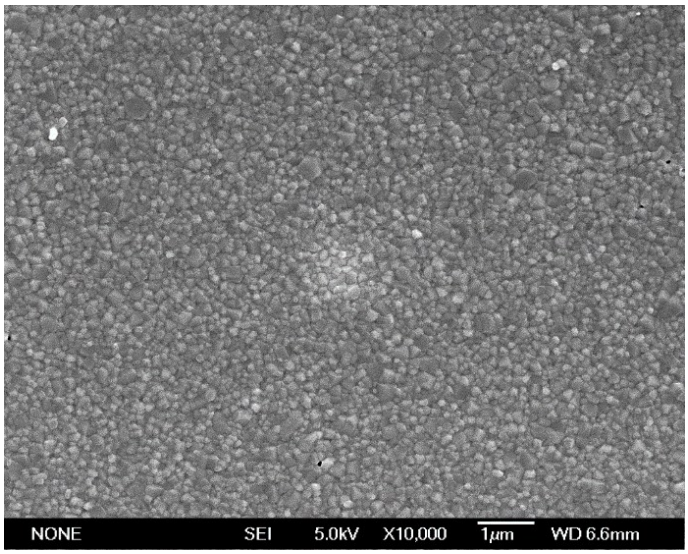

Figure S10. Typical SEM image of $CH_3NH_3PbI_3$ perovskite thin film.

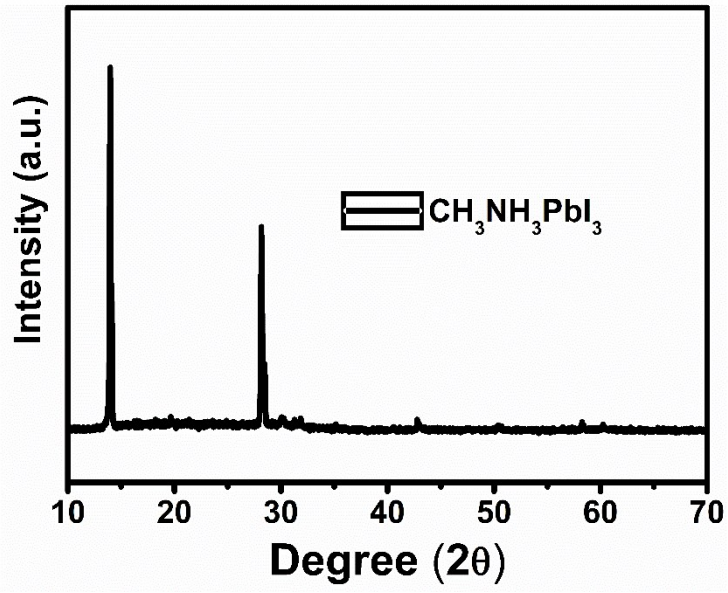

Figure S11. X-ray diffraction pattern of $CH_3NH_3PbI_3$ perovskite thin film used in this work.

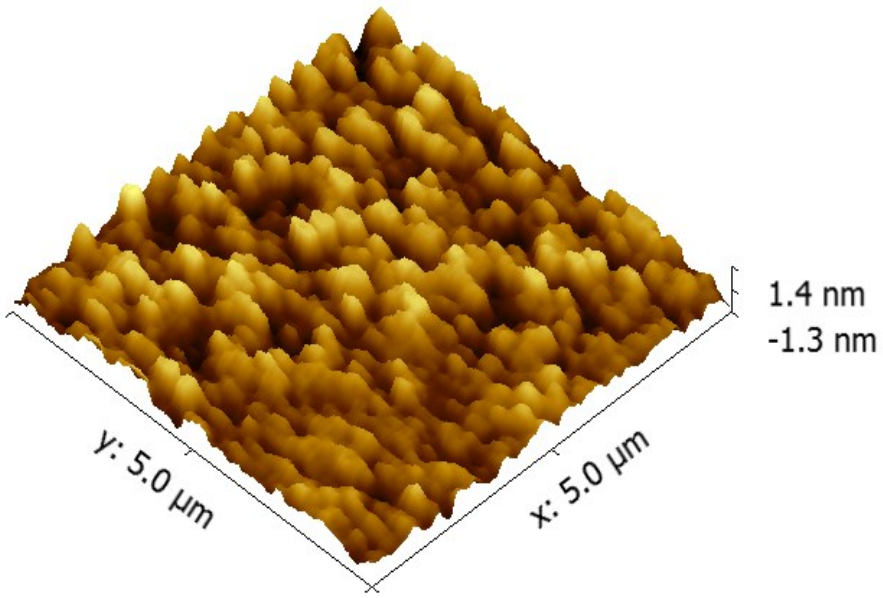

Figure S12. Three-dimensional AFM image of bilayer perovskite/**TDTP** thin film.

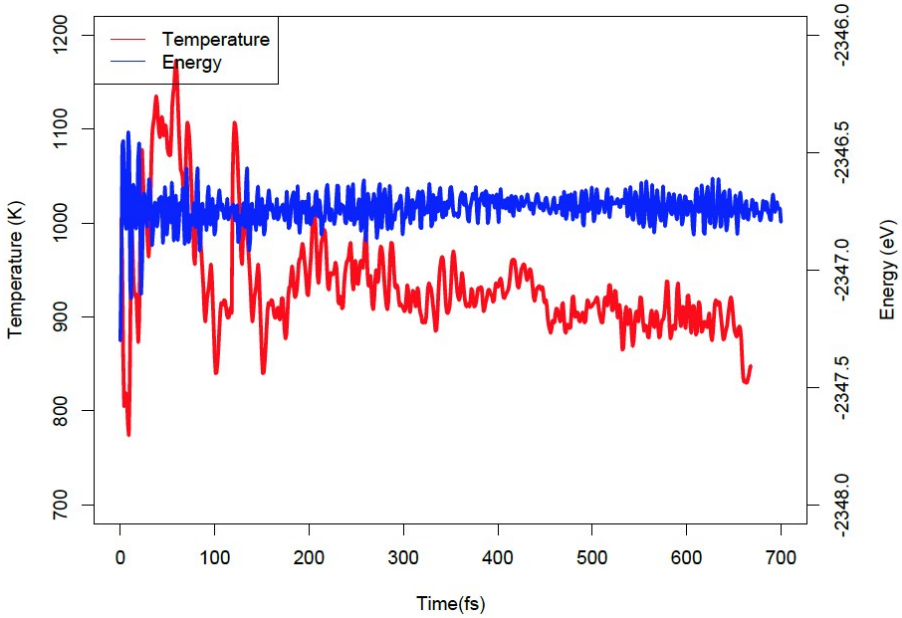

Figure S13. Temperature and energy of a PYPH molecule on a 4 ×4 110-perovksite surface in MD simulation.

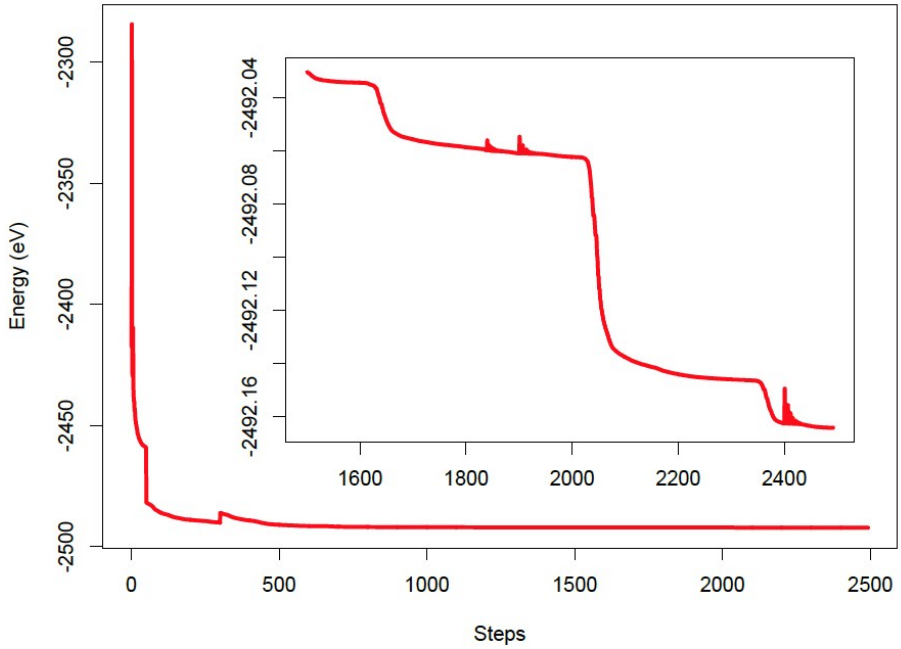

Figure S14. The energy of a PYPH molecule on a 4 ×4 110-perovksite surface in geometry optimizing simulation.

Table S1. Experimental electronic properties of **TDTP** and **PYPH**.

Compounds	E_{LUMO} (eV)[a]	E_{HOMO} (eV)[b]	E_{gap} (eV)[c]
TDTP	-4.03	-5.44	1.41
PYPH	-3.92	-5.80	1.88

[a]From CV: $E_{LUMO} = -[4.8-E_{Fc} + E_{re/onset}]$ eV (E_{Fc}= 0.24 V).[b]$E_{HOMO} = E_{LUMO} - E_g^{opt}$.[c]from UV-vis.

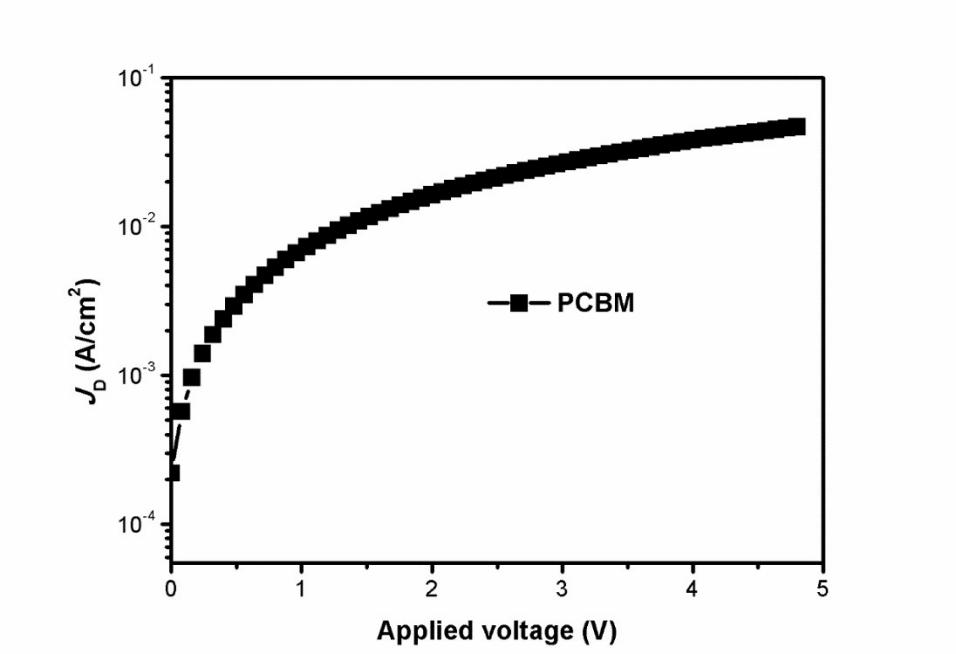

Figure S15. *J-V* curve of electron-only device with a device structure of Glass/ITO/Al/PCBM/Ca/Al.

Reference

1. P.-Y. Gu, J. Zhang, G. Long, Z. Wang, Q. Zhang, *Journal of Materials Chemistry C*, **2016**, *4*, 3809 - 3814.